PHOSPHOGYPSUM WASTE LIME AS A PROMISING SUBSTITUTE OF COMMERCIAL LIMES: A RHEOLOGICAL APPROACH

M.I. Romero-Hermida [a], A.M. Borrero-López [b], F.J. Alejandre [c], V. Flores-Alés [c (*)], A. Santos [d], J.M. Franco [b], L. Esquivias [a]

[a] Dpt. Física de la Materia Condensada, Universidad de Sevilla.

Avda. Reina Mercedes s/n, 41012 Sevilla, Spain.

[b] Pro^{2}TecS – Chemical Product and Process Technology Center. Dpt. Ingeniería Química. Universidad de Huelva.

Campus de "El Carmen". Universidad de Huelva. 21071 Huelva. Spain.

[c] Dpt. Construcciones Arquitectónicas II, Universidad de Sevilla.

Avda. Reina Mercedes nº4, 41012 Sevilla, Spain.

[d] Dpt. de Ciencias de la Tierra, Universidad de Cádiz.

Campus Universitario de Pto. Real 11519, Puerto Real, Cádiz, Spain.

(*) CORRESPONDING AUTHOR. Email vflores@us.es

ABSTRACT

This paper presents the rheological properties of three types of lime putty, specifying the influence of their origin. The study aims to compare a special lime putty prepared from phosphogypsum with a commercial lime powder and an aged lime putty. The results obtained in terms of chemical composition, crystalline structure, grain size and rheological characterization, (linear viscoelasticity, shear rate and time-dependent flow behaviour) are presented in the study.

Putties studied present a similar rheological response, which mainly depends on the particle size and water content. Lower values of the linear viscoelastic functions and viscosity were found for the phosphogypsum lime putty, in agreement with the higher particle size. Transient flow tests reveal a predominant elastic response with no significant shear-induced structural perturbations. However, either a thickening phenomenon over time, i.e. rheopexy, favoured at

low shear rates, or a viscosity decrease, i.e. thixotropy, favoured at high shear rates, was observed.

KEY WORDS: phosphogypsum; carbonatation; lime, rheology

1. INTRODUCTION

The fertilizer manufacturing industry in the province of Huelva (SW Spain) is based on an important production of phosphoric acid by a wet processing of the phosphoric rock, formed mainly by the apatite mineral ($Ca_5(PO_4)_3OH$)), with sulphuric acid. An industrial waste called phosphogypsum (PG) results from this process, which is mainly composed of calcium sulphate dihydrate [1]. The PG is taken to a suspension with water and pumped to storage rafts, where it decants and dries out. Currently, the material stored reaches 120 million tons and occupies an area of 1,200 hectares in a marsh area near the estuary formed by the union of the Tinto and Odiel river mouths(Fig.1) [2].

This waste, in whose composition appears toxic metallic impurities and radionuclides of natural origin, has been accumulated over the years in the open air with the consequent social and environmental conflicts. The radionuclides content of this waste makes it be considered as "Naturally Occurring Radioactive Material" (NORM). In particular, this waste concentrates important quantities of isotopes such as ^{226}Ra, ^{238}U, ^{230}Th and ^{210}Pb-^{210}Po, which precipitate with phosphogypsum due to their similarity with calcium [3] and whose presence must be considered in its management and treatment [4,5].

In such scenario, it is crucial to find alternatives for a better PG waste management. In the context of the need to advance in a scientific technology that allows its treatment as a by-product for other industrial processes, a simple procedure has been developed by treating the PG with a sodium hydroxide solution, obtaining sodium sulphate and a precipitate of slaked lime (portlandite) [6,7].

This reaction has a double advantage, on the one hand, it causes the precipitation of the isotopes present in the PG and, on the other hand, it provides lime putty as resulting by-product, with interest for the construction industry. Previous results have shown a high performance in the

precipitation reaction of calcium hydroxide and the transfer of impurity traces to the solid product, so that an interesting degree of stabilization is achieved, compared to the danger posed by their presence in the fluid state with the consequent risk derived from leaching [8]. An additional advantage of this process is the great potential capacity of carbonation of the hydroxide obtained, representing a positive environmental contribution due to the mineral sequestration of CO_2 from a potentially hazardous waste.

In terms of application, the plasticity of the pulps obtained from the industrial process described is a very important factor in the possible use as a substitute for conventional commercial putties. The viability of the product obtained to be incorporated into mortars or used as a paste in construction applications requires an adequate workability, similar to that of the products usually employed. Therefore, the correct knowledge of the rheological behaviour, in comparison with similar products that can be found in the market, is necessary before validating any possible application. The concept of workability of the products obtained is closely linked to the particle size and size distribution, to the extent that this size distribution of the portlandite crystals influences the viscosity of lime suspensions.

A correct assessment of the rheological behaviour of lime putty needs to comprise the analysis of both the linear viscoelastic and viscous flow responses, the latter including possible shear rate and time effects (thixotropy or rheopexy), which represent the mechanical behaviour under static and stressed conditions, respectively. In general, full rheological characterizations of lime putty are scarcely found in the literature, normally limited to the flow behaviour. In most cases, these studies reveal a shear-thinning behaviour for lime putty [9,10], where the apparent viscosity is mainly dependent on particle size and consequently on particle volume fraction [11-15]. In addition, some studies pointed out a yielding flow behaviour [9,16], with a characteristic yield stress which can be estimated by fitting the flow curve to the Bingham model [9,17]. However, in most of these studies the shear rate range applied is certainly limited to extrapolate a feasible yield stress value. On the other hand, the time dependence under shearing must be

evaluated in order to be correlated with the workability and possible applications [18]. The time-dependent flow behaviour can be studied by means of shear rate hysteresis loops [9,12] or, preferably, stress (or viscosity) growth curves at constant shear rate [11,13,15]. Regarding transient flow properties, some controversy and contradictory results can be found in the literature, obtaining both thixotropic and rheopectic behaviours depending on the type of lime putty and processing [8,12,16]. Regarding the linear viscoelastic response, only a few studies reported the dynamic viscoelastic moduli as a function of stress (or strain) amplitude, in order to determine the extension of the linear viscoelasticity regime [11], or as a function of time at constant amplitude [16], where a predominant elastic behaviour was apparent for different lime putty.

Figure 1. Location map of the phosphogypsum storage rafts (Source: Google Maps)

The object of this work is focused on the rheological characterization of a lime putty obtained as a by-product from the treatment of phosphogypsum waste with a solution of Na(OH). It has been named as lime putty from phosphogypsum (PLP). Together with this, the rheological properties and granulometries have been compared with those of two similar commercial products: a commercial lime putty with five years of aging, designed as aged lime putty (ALP), and another lime putty made in the laboratory from a commercial lime powder (LLP).

2. METHODOLOGY

2.1 Crystal morphology. A parameter

Portlandite is formed by precipitation [19] giving rise to hexagonal sheets with a perfect basal exfoliation. It is possible to make a study of the predominant morphology in these crystals (prismatic and planar) of portlandite oriented aggregates, comparing the Relative intensities of the previous reflections using parameter A (0001) [20].

$$A(0001) = \frac{I(0001)}{I\,(1011)}$$

I (0001) intensity (integrated area of each peak) of the reflection at 2θ = 18º

I (1011) intensity (integrated area of each peak) of the reflection at 2θ = 34º

The second one is usually of higher intensity with respect to the first one.

Several authors have indicated that parameter A (0001) indirectly gave a degree of the evolution or aging of lime putty [21-23], in such a way that the higher the value of A, there are more portlandite crystals in the form of platelets, since as they age the originally prismatic crystals separate into thinner hexagonal plates, said separation occurs along the planes (0001), which are the planes of exfoliation of said mineral.

2.2 X-ray fluorescence and X-ray diffraction

For the PLP sample, the major and minor chemical components of the plaster were analysed by X-ray fluorescence (XRF) using an Axios Panalitycal spectrometer. The sample characterization was continued with the identification of the mineralogical phases by X-ray powder diffraction (XRD) using a Bruker-AXS D8 Advance diffractometer equipped with copper anode Cu Kα (λ=1.5405Å), with a Bragg-Bentano θ-θ configuration, a nickel filter, and a LynxEye linear detector, and the XRD patterns were obtained using the powder technique, at an angle of 2θ, a range of 3º to 70°, and a 0.03° step scan with a 1s step.

2.3 Granulometry

The morphology of the different lime putty samples was characterized by field-emission gun scanning electron microscopy (SEM-FEG), with a Hitachi S5200 microscope, at 5 kV accelerating voltage.

The granulometric analysis was performed by laser diffraction in a Malvern Mastersizer equipment which allows to know the particle sizes and the granulometric distribution of wet dispersions according with the working real conditions as putties. Granulometric distribution of crude solid phosphogypsum sample (PG) was also determined in dry dispersions.

The following protocol for wet dispersions based on that proposed by Rosell (2013) has been followed [24]:

A small sample aliquot is placed in a beaker where it is dispersed in a small amount of distilled water to homogenize the sample, and then placed in an ultrasound bath at maximum intensity to avoid particle agglomeration. The ultrasonication time applied in different experiments was 5 min (42 KHz). A certain amount of the already homogenized sample was pipetted and dispersed with a shaker, at a speed of 2500 rpm, in a bucket with 100 ml of distilled water. Once the system was stabilized, particle size distribution was read through the equipment software and the results were recorded twice consecutively, using the average of the measurements as the final result.

The adjustment parameters of the Mastersizer were: a) Dispersing water with refractive index RI = 1.33, b) Reflection rate: 1.5; c) Absorption index: 0.01. The theoretical models applied on data analysis are those defined by Fraunhofer and Mie, considering that the first of them is more in line with theoretical models of confirmation of spherical particles and the second, to elongated particles.

The statistics of the distribution are calculated by the equipment from the results obtained using the derived diameters d(m,n), an internationally agreed method of defining the mean and other moments of particle size:

$$d(m,n) = \left[\frac{\sum V_i (d_i)^{m-3}}{\sum V_i (d_i)^{n-3}}\right]^{\frac{1}{m-n}}$$

$$d(m,n) = \left[\frac{\sum V_i (d_i)^{m-3}}{\sum V_i (d_i)^{n-3}}\right]^{\frac{1}{m-n}}$$

where V_i is the relative volume in class i with mean class diameter of d_i, d(0,5), d(0,1) and d(0,9) are standard percentile readings from the analysis: d(0, 5) is the median of the volume distribution, d (0,1) is the size of particle below which 10% of the sample lies and d(0,9) is the size of particle below which 90% of the sample lies. d(4,3) is the Volume Weighted Mean or Mass Moment Mean Diameter and d(3,2) is the Surface Weighted Mean, also known as the Surface Area Moment Mean Diameter or Sauter mean.

2.4 Thermogravimetric analysis (TGA)

Thermogravimetric analysis aimed to determine water content of the different lime putty studied. They were performed using a Q50 (TA Instrumets, Water, USA) apparatus following a constant increase of 10ºC/min up to 600ºC starting at room temperature (around 20ºC).

2.5 Rheological tests

Each putty was rheologically analysed at four diverse water contents, i.e. 45, 50, 60 and 70%. LLP samples were directly obtained by dispersing the dry powder in distilled water up to the desired concentration. Nonetheless, as phosphogypsum and aged limes were hold in pastes with around 50% water content, TGA was used to determine the exact content of water in order to adjust with distilled water the desired concentration. To obtain lower water concentrations (45

and 50%), a certain amount of water was previously removed by centrifugation of the limes, performed during 15 minutes at 4200 rpm, and then the same protocol for the adjustment of concentration was followed. The purpose of using centrifugation to decrease the initial water content is to avoid any alteration that the drying process in a stove might produce in limes crystallinity.

For each lime sample, stress growth experiments in transient shear flow, at four selected shear rates, i.e., 0.1, 1, 10 and 100 s^{-1}, were performed in a controlled-strain ARES rheometer (Rheometric Scientific, U.K.) fitted with a special mixing geometry dealing with a cylindrical vessel and a helical ribbon very convenient to avoid particle sedimentation and wall slip effects during the measurement [25]. These tests allow to monitor the evolution of the viscosity with shearing time. Moreover, viscous flow measurements were also obtained by applying a shear rate-stepped ramp from 0.03 to 100 s^{-1}, waiting time of 2 min in each step, using the same vane geometry. On the other hand, small-amplitude oscillatory shear (SAOS) tests within the linear viscoelastic regime were carried out in a MARS (Haake, Thermo Scientific, Germany) rheometer, using a 50 mm parallel serrated plate-plate geometry, in a frequency range of 0.03-100 rad/s. The linear viscoelastic range was previously determined by means of stress sweep tests at 1 Hz. All rheological measurements were performed as soon as samples were prepared, in order to obtain reliable results according to the different concentrations.

3. PHOSPHOGYPSUM AND LIME PUTTIES CHARACTERIZATION RESULTS

3.1 Lime putty from phosphogypsum (PLP)

3.1.1 Raw material

Crude solid and dried phosphogypsum (~ 96% by weight of $CaSO_4 \cdot 2H_2O$) was supplied by Fertiberia (Huelva, Spain). The PG was homogenized, ground and dried in the oven at 40°C for

48 hours to preserve the structural water of gypsum. The diffraction patterns (Fig. 2) denote a very homogeneous composition as expected in relation to the crystalline phases present in the sample, mostly gypsum (around 96%), presenting a small residual fraction of quartz that comes from the storage of the residue in the rafts. A more detailed composition was determined by XRF. The PG sample is composed mainly of Ca and S, in a molar ratio very close to the unit (0.993), as expected for the gypsum, and a 18.4% by weight loss of ignition (LOI), due to dehydrated gypsum (table 1). The particle size distribution of phosphogypsum dried in the oven at 40ºC to eliminate the humidity, without the application of any other treatment, was determined by laser granulometry dry way to completely characterize this material. It shows a granulometric profile with a very homogenous distribution of sizes with 90% of particles smaller than 108.023 microns, 50% below 33.026 μm and 10% of 5.158 μm. SEM observations reveal the presence of gypsum crystals (Fig. 3). The phosphogypsum has a very marked crystalline structure, mainly of rhomboidal and hexagonal forms. In our case, we observed a stacking arrangement of homogenous and prismatic phosphogypsum and a well-developed euhedral structure, monoclinic with a tabular habit of rhombic and orthorhombic crystals [26].

Figure 2: X-ray diffraction patterns of samples “PG”,

Figure 3: SEM images of sample “PG”

3.1.2 Synthesis of the PLP

The process used to obtain lime putty is based on the method proposed by Cárdenas-Escudero [6], even though some modifications have been made regarding its initial methodology. In a first stage, 300 g of phosphogypsum were dissolved in 500 ml of distilled H_2O under magnetic stirring, obtaining a suspension after stirring. On the other hand, a 9M alkaline solution of NaOH (PA-ACS-ISO pellets, PANREAC Química SAU, 98% chemical purity) was slowly added to this suspension to favour the crystallization of the solid phase. The mixture was kept

under atmospheric pressure and at room temperature under magnetic stirring for approximately 10 min (Fig. 4). The chemical reaction associated with this chemical process is described below:

$$CaSO_4 \cdot 2H_2O + 2NaOH \rightarrow Ca(OH)_2 + Na_2SO_4 + 2H_2O$$

This process results in the dissolution of the PG and the precipitation of an off-white solid phase labelled "PLP" and a Na_2SO_4 solution as a clear supernatant liquid. The solid phase "PLP" was obtained by centrifugation during 5 min at 3000 rpm and taken for XRD (Fig. 5) and XRF (table 1) analysis; whereas the liquid phase was discarded since it was not the object of our study. Several samples of the solid phase were taken for study. The samples were dried at 40ºC and kept in hermetic containers to avoid their carbonation.

As a result, a precipitate of a whitish solid phase $Ca(OH)_2$ and an aqueous phase with a high concentration in Na_2SO_4 were obtained. In order to not alter as much as possible the lime putty obtained, once the precipitation was completed, the supernatant liquid was removed and the solid phase washed with distilled water to reduce the concentration of sulphates in the sample. The process of obtaining the lime putty ends with the incorporation of barium hydroxide to achieve complete insolubilization of the sulphates present in the precipitate so as to avoid the interferences that could result from the crystallization/dissolution of these salts. The final product obtained is a lime putty with an approximate humidity of 50%.

Figure 4: Experimental process scheme

Figure 5: X-ray diffraction pattern of simple “PLP”

Regarding PLP composition shown in Table 1. Chemical analysis results are in agreement with the major presence of portlandite and minorities of thenardite and quartz which can be appreciated in DRX spectrum. The major presence of CaO, attributable to calcium hydroxide,

Na_2O and SO_3 assignable to sodium sulphate can be appreciated, which would lead to an approximate composition of around 65% of portlandite and 30% of sodium sulphate, with the presence of silica impurities attributable to quartz and phosphates (1.02% P_2O_5).

Table 1: Major elements chemical composition. (LOI: Loss of ignition at 1000 ºC; ND: not detected).

Major elements (wt.%)	Phosphogypsum	PLP
SiO_2	2.52	4.09
Al_2O_3	0.20	0.12
Fe_2O_3	ND	ND
MnO	ND	ND
MgO	ND	ND
CaO	32.00	49.41
Na_2O	0.01	12.43
K_2O	0.02	ND
TiO_2	ND	ND
P_2O_5	0.65	1.02
SO_3	46.00	13.56
Cl	ND	ND
F	ND	ND
SrO	ND	ND
BaO	ND	ND
LOI	18.40	19.40

In relation to other elements present in the phosphogypsum, Cr, As, T, Ni, V, Se, Cd, Pb, Zn and Th have been analysed [27]. Most of these impurities were transferred in the process to the resulting slaked lime (portlandite), being practically undetectable in the supernatant liquid. The concentrations in the portlandite of most of the trace impurities initially contained in the

phosphogypsum implied average transfer factors of 100%, so most of these elements would be fixed [28]. It should be noted that the precipitation of heavy metals with greater contaminating capacity occurs in the resulting solid product, which is positive as they are stabilized, decreasing the risks of solubilization and leaching [29].

3.2 Other lime putties

Two other lime putties were characterized and taken as reference:

- Lime putty CL90-S PL, which follows UNE-EN 459-1:16, manually slaked and aged for five years in raft, was supplied by the company Gordillo's de Morón de la Frontera (Seville) (ALP). The supernatant liquid has been eliminated by decanting, so that drying by heating the sample is avoided, avoiding alteration of the natural crystallization process of the portlandite, obtaining a concentration similar to the product coming from the treatment of the phosphogypsum. One sample was dried in an oven at 40ºC and was taken for analysis by XRD (Fig. 6). The majority phase is portlandite, calcite peaks are visibly attributable to the sample handling process
- The hydrated calcitic lime CL90-S was supplied in powder form by Gordillo's and then it was used to prepare a lime putty in laboratory with a water:lime powder weight ratio of 0.5 (LLP). It was prepared by stirring until the product was completely homogenized, dried in an oven at 40ºC, A sample was dried in an oven at 40ºC and was taken for analysis by XRD (Fig. 7). The majority phase is portlandite, whereas calcite peaks are visible and attributable to the sample handling process.

Figure 6. Diffractograms and crystalline phases in the sample “ALP”

Figure 7. Diffractograms and crystalline phases in the sample "LLP"

4. RESULTS AND DISCUSSION

The results obtained from the putties granulometric analysis in water, with or without ultrasound treatment (0, 5 min time of exposure) with different approximations are shown in Fig. 8, 9, 10 and tables 2 and 3. We have used both Fraunhofer and Mie difraction approaches to calculate the particle size distribution. Fraunhofer´s does not require the knowledge of the optical properties of the sample, whereas Mie´s does (refractive index and imaginary component) together with the refractive index of the dispersant.

PLP SEM-FEG micrographies show an abundance of portlandite hexagonal crystals of tabular morphology (size ~ 1µm), very regular and well organized (Fig. 11 top). There are signs of lamination in the direction parallel to (0001). In addition, portlandite characterized by platy nanoparticles (needle and sheet forms), forming micrometric aggregates with high porosity (Fig.11 middle), and submicrometer platelets, crystalline nanoparticles of portlandite are observed (Fig.11 bottom).

The results obtained by granulometry indicate that the particle sizes are higher than those determined by SEM-FEGL, which may be a consequence of an important phenomenon of agglomeration of lime particles in the aqueous phase, with a decisive influence over the rheological behaviour. These differences are confirmed by the significant decrease in particle size in all the percentiles when the measurement is made by applying ultrasonication. It is important to point out that, regardless of the influence of the ultrasonication treatment, the three samples behaviour evolves in a similar way, which guarantees a correct correlation with the rheological characterization. In any case, it should be noted that PLP sample has a mean particle

size higher than ALP and LLP, which allows to associate a slightly more fluid behaviour associated with lower specific surface area and lower number of micro-particles [11-15,23].

Figure 8: (top) approximation of Fraunhofer for PLP and (bottom) approximation of Mie for PLP.

Figure 9: (left) approximation of Fraunhofer for LLP and (right)approximation of Mie for LLP.

Figure 10: (left) approximation of Fraunhofer for the ALP and (right)approximation of Mie for the ALP.

Table 2. *Percentiles and lime particle sizes scattered in water. Approximation of Fraunhofer*

Ultrasonication duration (min)	Percentil PLP (µm)	Percentil LLP (µm)	Percencil ALP (µm)
0	d(09)=99.725 d(05)=42.584 d(01)=14.926	d(09)=191.779 d(05)=26.755 d(01)=6.716	d(09)=374.463 d(05)=38.481 d(01)=10.295
5	d(09)=72.091 d(05)=30.516 d(01)=11.353	d(09)=50.293 d(05)=20.264 d(01)=6.336	d(09)=56.408 d(05)=14.977 d(01)=3.942

Table 3: *Percentiles and lime particle sizes scattered in water. Approximation of Mie.*

Ultrasonication duration (min)	Percentil PLP (µm)	Percentil LLP (µm)	Percentil ALP (µm)
0	d(09)=109.044 d(05)=45.857 d(01)=15.836	d(09)=202.051 d(05)=29.306 d(01)=7.779	d(09)=391.552 d(05)=40.555 d(01)=10.966

5	d(09)=71.57 d(05)=30.204 d(01)=11.824	d(09)=49.611 d(05)=20.819 d(01)=9.057	d(09)=60.460 d(05)=15.404 d(01)=5.581

Figure 11. SEM images of simple putty prepared from PLP. (top), LLP (middle) and ALP (bottom)

4.1 Viscoelastic behaviour

Fig. 12 shows the evolution of both storage (G') and loss (G") moduli with frequency for the different lime putty and water contents evaluated. As can be seen, as expected, the values of both viscoelastic moduli increase with solid content. Moreover, regarding the frequency dependence, at low water contents (typically 45 and 50%), the beginning of the terminal region, characterized by a crossover point between both viscoelastic functions, which determines the flow region, can be clearly observed at low frequencies for all putty samples, along with the plateau region, characteristic of three-dimensional internal structure resulting from interacting particles, at higher frequencies. Nonetheless, interestingly, when increasing water content, the plateau region is generally expanded in detriment of the terminal zone which was only detected at lower water contents. In principle, this is an unexpected result that may be explained by an enhancement of inter-particles interactions and therefore material cohesion as a result of increasing hydrogen bonding and capillary forces [30].

Figure 12. Viscoelastic moduli for LLP, ALP and PLP limes at different water concentrations.

When comparing the three lime putties at any given concentration, the highest values of SAOS (Small-Amplitude Oscillatory Shear) functions were shown by ALP, followed by LLP, excepting G" for the 45% water content (LLP45 and ALP45 samples), whereas PLP always

exhibited noticeably lower values of the viscoelastic functions. These results can be, in part, explained attending to the granulometry of the samples. The mean particle size of lime suspensions, generally varies inversely with the viscoelastic moduli, i.e. higher particle size leads to a lower structuration as a consequence of the lower number of interacting particles and specific surface area exposed. As previously mentioned, viscoelastic moduli decreased when water concentration was risen, however, there are significant differences among these drops when comparing the different limes. For instance, the differences respecting the aged lime which shows the highest values, became higher and higher when increasing water content. These relative progressions are illustrated in table 4 for the storage moduli at 10 rad/s. Finally, the relative elasticity of the different samples can be evaluated by means of the loss tangent (tan δ = G"/G'). As can be seen in Fig. 13, the values and evolution of the loss tangent with frequency are generally similar for all the samples, independently on the type of lime and water content. Nevertheless, some interesting points can be remarked. For ALP, a lower tan δ was obtained for ALP45, which could be expected as it is the most concentrated sample. However, the lowest values of tan δ for LLP were shown by LLP70, in agreement with the more extended plateau region. The same influence can be observed in PLP70 at low frequencies.

Table 4. Percentage difference of G' values, at 10 rad/s, respecting the aged lime putty (ALP).

Water content (%)	LLP (%)	PLP (%)
45	-9.75	-44.70
50	-58.16	-82.90
60	-79.00	-88.71
70	-85.31	-95.99

Figure13. tanδ for LLP, ALP and PLP at different water concentrations.

4.2 Viscous flow measurements

All samples demonstrated a shear-thinning behaviour at all the concentrations studied within the shear rate range studied, however, there are several differences among the different lime kinds regarding the viscosity values and shear rate dependence (Fig. 14). For most of the samples, the evolution of viscosity can be properly fitted to the power-law model, as reported elsewhere [9]:

$$\eta = K \cdot \dot{\gamma}^{n-1}$$

where K and n are the consistency and flow indexes respectively. Values of these fitting parameters are listed in table 5. In all cases, the flow index was similar and close to zero, characteristic of yielding materials [31]. However, for 60 and 70% water contents, commercial and phosphogypsum lime putties shown a tendency to reach both zero- and high-shear rate limiting viscosities, which needs additional fitting parameters, as also found in other studies [15]. The Cross model can be satisfactorily employed to fit this evolution:

$$\eta = \eta_\infty + (\eta_0 - \eta_\infty)/(1 + (m \cdot \dot{\gamma})^{n-1})$$

where η_∞ and η_0 are the final and initial viscosity values, whilst m is related to reciprocal shear rate for the onset of the power-law evolution, and n has a similar meaning than the same parameter in the power-law model. Values of these parameters for these particular putties are also included in table 5.

Figure 14. Viscous flow measurements (filled points) for LLP, ALP and PLP limes at different water concentrations. (hollow points refer to equilibrium values obtained from stress growth experiments).

Table 5. Characteristics parameters of the power-law and Cross models for the lime putty studied.

Sample	Eta_0	Eta_∞	K($Pa \cdot s^n$)	m($Pa \cdot s^n$)	n
PLP45			27.56		0.07
PLP50			18.24		0.1
PLP60	44.37	0.03		62.22	0.06
PLP70	8.48	0.013		40.62	0.05
LLP45			105.67		0.15
LLP50			34.31		0.18
LLP60	103.48	0.09		15.27	0.07
LLP70	38.54	0.09		15.12	0.19
ALP45			321.02		0
ALP50			127.29		0
ALP60			34.32		0.04
ALP70			9.73		0.06

When the three lime putty samples are compared, again ALP clearly shows the highest viscosity values, whereas PLP samples always show the lowest values (see for instance K values in table 5). These results are in agreement with those previously discussed regarding the viscoelastic response. On the other hand, viscosity progressively decreases with the water content, following a power-law evolution, for all the lime putties studied. This fact supports that water dependent inter-particle interactions under flow for slaked limes are qualitatively similar. However, this decrease in viscosity is more dramatic for LLP and especially for PLP samples (Fig. 15).

Figure 15. Variation of the viscosity values at 1 s^{-1} with water content.

4.3 Transient flow

The transient flow behaviour of the three lime putties was investigated by performing stress growth experiments at constant shear rates. Fig. 15 shows the transient flow curves, in the form of viscosity vs. time plots as a function of the applied shear rate, for all the samples studied. The evolution of the transient shear stress is similar to that observed for other thixotropic colloidal suspensions [32], which is the result of a well-known non-linear viscoelastic response initially, and the time-dependent shear-induced structural modification once the maximum shear stress, i.e. the stress overshoot, was reached. In most cases, the elastic deformation is the prevailing component, so that the stress overshoot, which was attained in seconds, approximately coincides with the equilibrium (steady-state) value, especially at highest water contents (60 and 70%), as can be seen in Fig. 15 in terms of viscosity. This means that no significant shear-induced structural perturbations occur over time. However, a much more complex behaviour is apparent at lower water contents. Thus, once the maximum value was attained, either a thickening phenomenon over time, i.e. rheopexy, favoured at low shear rates, or a viscosity decrease, i.e. thixotropy, favoured at high shear rates, was observed. This shear rate dependent behaviour found in highly concentrated putty may be explained as the result of a balance between a curing kinetics and the shear-induced disruption of aggregates. Exceptionally, both phenomena can be clearly distinguished, see for instance sample LLP50 at low shear rates. Moreover, some disturbances at high shear times and/or sudden drops in viscosity can be occasionally detected (see for instance samples LLP45 and ALP45 at relatively high shear rates), which must be attributed to shear-induced fracture phenomena.

A quantification of the shear-induced structural breakdown can be done by estimating the "amount of overshoot", which is defined as:

$$S^{+} = \frac{\tau_{max} - \tau_{\infty}}{\tau_{\infty}}$$

where τ_{max} is the stress overshoot and τ_{∞} is the equilibrium stress. Considering that, in most cases, almost constant values of the stress were reached before agglomeration or other mentioned anomalous effects, the equilibrium values here considered do not take into account those effects. The values of the amount of overshoot are shown in table 6 as a function of shear rate for all the samples studied. As can be seen, in general, very small values were obtained in all the samples, which corroborates that the viscoelasticity is the prevailing component and no significant structural breakdown is noticed. To support this fact, the equilibrium viscosity values obtained from the stress-growth tests were also added to Fig. 14 and compared with viscous flow curves obtained in stepped-stress ramps. As depicted in the figure, these values are reasonably in agreement for all the samples and concentrations studied.

By analogy with the amount of overshoot, another parameter more related with the applications of lime putty may be defined, considering the stress value at 1 min instead of the equilibrium one, which may be considered an approximate time for its stabilization:

$$S^{+}_{1min} = \frac{\tau_{max} - \tau_{1min}}{\tau_{1min}}$$

In this way, all the above-mentioned phenomena can take place at this time (1 min).. Either important negative values of this parameter (down to around -30% or -50%) or noticeable positive values can be indistinctly found, especially at low water contents and/or low shear rates, which is attributable to disruption, agglomeration and other effects previously discussed. The values of S^{+}_{1min} are also shown in table 6.

Figure 16. Transient Flow behaviour of the three lime putties studied and all water concentrations (Shear rates of 0.1 s^{-1} (■), 1 s^{-1} (●), 10 s^{-1} (▲), 100 s^{-1} (▼)).

Table 6. S^{+}_{eq} and S^{+}_{1min} for the samples studied.

	Shear rate (s^{-1})	S_{eq}	S_{1min}		Shear rate (s^{-1})	S_{eq}	S_{1min}		Shear rate (s^{-1})	S_{eq}	S_{1min}
PLP45	0.1	0.16	-0.58	LLP45	0.1	0.08	-0.38	ALP45	0.1	0.34	-0.34
	1	0.36	0.24		1	0.30	-0.28		1	0.74	-0.17
	10	0.00	-0.32		10	0.65	-0.36		10	0.20	0.48
	100	0.10	0.11		100	0.05	0.17		100	0.10	0.35
PLP50	0.1	0.10	0.10	LLP50	0.1	0.84	0.25	ALP50	0.1	0.46	-0.19
	1	0.00	0.00		1	1.02	0.51		1	0.75	0.00
	10	0.04	0.00		10	0.03	0.16		10	0.10	0.09
	100	0.05	0.03		100	0.21	0.14		100	0.01	0.01
PLP60	0.1	0.09	-0.37	LLP60	0.1	0.16	-0.15	ALP60	0.1	1.08	0.37
	1	0.08	-0.13		1	0.03	0.05		1	0.82	0.49
	10	0.09	0.06		10	0.56	-0.28		10	0.04	0.13
	100	0.18	0.15		100	0.02	0.02		100	0.03	0.02
PLP70	0.1	0.02	-0.13	LLP70	0.1	0.00	-0.04	ALP70	0.1	0.00	-0.04
	1	0.17	0.09		1	0.06	-0.03		1	0.09	0.13
	10	0.24	0.12		10	0.13	0.09		10	0.12	0.13
	100	0.02	-0.04		100	0.00	-0.01		100	0.02	0.01

5. CONCLUSIONS

The article herein presents the rheological behaviour of a commercial lime putty, and aged lime putty and a putty obtained from phospogypsum wastes of the Huelva province, confirming that PLP does not show any inappropriate behaviour regarding either linear viscoelasticity or viscous flow behaviour focused on possible applications as commercial-lime substituent in composite materials for the building and construction industry. In addition, the slaked lime

obtaining process from phospogypsum would consequently lead to the precipitation of hazardous isotopes, removing those from the liquid state where their presence put into risk both human being and the environment. Another powerful advantage is the high carbonation capacity that the slake limes possess, favouring CO_2 sequestration.

Generally, the transient flow behaviour was highly dependent on water content. The lime putties develop an initial viscosity increase (due to elastic effects) and afterwards either remains constant or slightly decreases, demonstrating a non-noticeable shear-induced structural change. Subsequently, at higher shearing times, two different anomalous behaviours can be found, especially at lower water contents: either a significant viscosity increase at low shear rates, which can be attributed to the formation of agglomerates, or a decrease in viscosity, predominantly at high shear rates, due to the disruption of aggregates or fracture occurrence. It is worth noticing that PLP, although exhibiting lower viscous values, displayed more stable and slightly thixotropic transient flow at high shear rates than ALP and LLP (comparable to stirring conditions of industrial putty application), avoiding the above explained anomalous effects, thus favouring the workability of this material.

Regarding frequency sweeps, all samples exhibit very similar qualitative response, being the elastic contribution more important than the viscous one, especially at high frequencies where the plateau zone is always noticed. This linear viscoelastic response confirms a high level of structural interactions among calcium hydroxide particles. Moreover, LLP and ALP samples shows very similar values of the SAOS functions at low water concentrations. Nonetheless, when water concentration was raised, differences became higher, ALP showing the highest values. On the contrary, PLP always exhibited the lowest values of the SAOS functions analysed for all concentrations studied.

Viscosity flow tests demonstrate a pronounced shear-thinning behaviour for all samples, with flow index values close to 0, PLP again showing the lowest viscosity values. In addition, the viscosity of PLP samples is more affected by water content.

All these rheological properties measured were consistent with the grain size of the samples studied. The portlandite crystals agglomeration phenomenon has a relevant influence on the rheological behaviour of the pastes, independently of the crystalline morphology. Attending to the granulometry, the larger the mean particle size, the lower the values of the linear viscoelastic functions and viscosity. Thus, a larger agglomeration particle size develops a smaller structuring effect due to the number of interacting particles and specific surface exposed. In this way, the PLP sample always showed lower viscoelastic functions values than commercial putties, in coherence with the granulometric curves.

ACKNOWLEDGEMENT

The authors would like to thank the aid of CITIUS at the University of Seville for the use of their laboratories for the characterization analyses. A.M.B.-L. has received a Ph.D. Research Grant from the Ministerio de Educación, Cultura y Deporte (FPU16/03697)

REFERENCES

[1] W. F. Chang, Engineering Properties and Construction Applications of Phosphogypsum, University of Miami Press, 1990.

[2] P. Bolivar, J.E. Martín, R. García-Tenorio, J.P. Pérez-Moreno, J.L. Mas, Behaviour and fluxes of natural radionuclides in the production process of a phosphoric acid plant, Appl. Radiat. Isot., 67 (2009) 345-356. https://doi.org/10.1016/j.apradiso.2008.10.012

[3] R. Pérez-López, J.M. Nieto, I. López-Coto, J.L. Aguado, P. Bolívar, M. Santisteban, Dynamics of contaminants in phosphogypsum of the fertilizer industry of Huelva (SW Spain):

from phosphate rock ore to the environment, Appl. Geochem. 25 (2010) 705-715. https://doi.org/10.1016/j.apgeochem.2010.02.003

[4] R. Periáñez, A. Martínez-Aguirre, M. García-León, U-and Th-isotopes in an estuarine system in Southwest Spain: tidal and seasonal variations, Appl. Radiat. Isotopes 47 (1996) 1121-1125.

[5] H. Tayibi, C. Gascó, N. Navarro, A. López-Delgado, F.J. Alguacil, F.A. López-Gómez, The radiological impact and restrictions on phosphogypsum waste applications. 1st Spanish National Conference on Advances in Materials Recycling and Eco-Energy, Ed. F.A. López, F. Puertas, F. J. Alguacil and A. Guerrero Madrid (2009) 71-74.

[6] C. Cárdenas-Escudero, V. Morales-Flórez, R. Pérez-López, A. Santos, L. Esquivias, Procedure to use phosphogypsum industrial waste for mineral CO2 sequestration, J. Hazardous Mat. 196 (2011) 431-435. https://doi.org/10.1016/j.jhazmat.2011.09.039

[7] M.I. Romero Hermida, V. Morales Flórez, A. Santos, Alberto, L.A. Villena, L. Esquivias, Technological Proposals for Recycling Industrial Wastes for Environmental Applications, Minerals 4 (2014) 746-757. https://doi.org/10.3390/min4030746

[8] M. Aoun, A.G. El Samrani, B.S. Lartiges, V. Kazpard, Z. Saad , Releases of phosphate fertilizer industry in the surrounding environment: Investigation on heavy metals and polonium-210 in soil, J. Env. Sciences 22 (2010)1387-1397. https://doi.org/10.1016/S1001-0742(09)60247-3

[9] A. Arizzi, R. Hendrickx, G. Cultrone, K. Van Balen, Differences in the rheological properties of calcitic and dolomitic lime slurries: influence of particle characteristics and practical implications in lime-based mortar manufacturing, Mat. Const. 62 (2012) 231-250. https://doi.org/10.3989/mc.2011.0311

[10] L.G. Baltazar, F.M.A. Henriques, F. Jorne, M.T. Cidade, The use of rheology in the study of the composition effects on the fresh behaviour of hydraulic lime grouts for injection of masonry walls, Rheol. Acta. 52 (2013) 127-138. https://doi.org/10.1007/s00397-013-0674-x

[11] A.F.N. De Azerêdo, G. Azeredo, A.M.P. Carneiro, Study of rheological parameters of lime-metakaolin paste made of kaolin wastes and lime paste, Key Eng. Mater. 668 (2015) 419-

432.

[12] M. Boháč, R. Nečas, The role of aging on rheological properties of lime putty, Procedia Eng. 151 (2016) 34-41. https://doi.org/10.1016/j.proeng.2016.07.355

[13] J.R. Rosell, S. Chinchón, L. Haurie, A. Navarro, I. Rodríguez, Características reológicas de pastas de cal, (2008). X Congreso Nacional de Materiales. San Sebastián.

[14] Y. Sébaïbi, R.M. Dheilly, M. Quéneudec, A study of the viscosity of lime-cement paste: Influence of the physico-chemical characteristics of lime, Constr. Build. Mater. 18 (2004) 653-660. https://doi.org/10.1016/j.conbuildmat.2004.04.028

[15] E. Ruiz-Agudo, C. Rodriguez-Navarro, Microstructure and rheology of lime putty, Langmuir 26 (2010) 3868-3877. https://doi.org/ 10.1021 / la903430z

[16] M. Fourmentin, G. Ovarlez, P. Faure, U. Peter, D. Lesueur, D. Daviller, P. Coussot, Rheology of lime paste - A comparison with cement paste, Rheol. Acta. 54 (2015) 647-656. https://doi.org/10.1007/s00397-015-0858-7

[17] C. Atzeni, A. Farci, D. Floris, P. Meloni, Effect of aging on rheological properties of lime putty, J. Am. Ceram. Soc. 87 (2004) 1764-1766. https://doi.org/10.1111/j.1551-2916.2004.01764.x

[18] H. Paiva, A. Velosa, R.Veiga, V.M. Ferreira, Effect of maturation time on the fresh and hardened properties of an air lime mortar, Cem. & Conc. Res. 40 (2010) 447-451. https://doi.org/10.1016/j.cemconres.2009.09.016

[19] V.S. Harutyunyan, A.P. Kirchheim, P.J.M. Monteiro, A.P. Aivazyan, P. Fischer, Investigation of early growth of calcium hydroxide crystals in cement solution by soft X-ray transmission microscopy, J. Mater. Sci. 44(2009) 962-969. https://doi.org/10.1007/s10853-008-3198-5

[20] R. Datwiler, P.J.M. Monteiro, H.R. Wenk, Z. Zhong, Texture of calcium hydroxide near the cement paste-aggregate interface, Cem. & Conc. Res. 18 (1988) 823-829. https://doi.org/10.1016/0008-8846(88)90109-3

[21] C. Rodriguez-Navarro, E. Hansen, W.S. Ginell, Calcium hydroxide crystal evolution upon aging of lime putty, J. Am. Ceram. Soc. 81 (1998) 3032-3034. https://doi.org/10.1111/j.1151-2916.1998.tb02735.x

[22] G. Mascolo, M.C. Mascolo, A. Vitale, O. Marino, Microstructure evolution of lime putty upon aging, J. Cryst. Growth 312 (2010) 2363-2368. https://doi.org/10.1016/j.jcrysgro.2010.05.020

[23] M.G. Margalha, A.S. Silva, M.D.R. Veiga, J.D. Brito, R.J. Ball, G.C. Allen, Microstructural changes of lime putty during aging, J. Civil Eng. 25 (2013) 1524-1532. https://doi.org/10.1061/(ASCE)MT.1943-5533.0000687

[24] J.R. Rosell, Aportaciones al conocimiento del comportamiento deformacional de pastas de cal.tamaño y formas de las partículas y su viscosidad, Tesis doctoral UPC (2013) Barcelona.

[25] H.A. Barnes, A review of the slip (wall depletion) of polymer solutions, emulsions and particle suspensions in viscometers: its cause, character, and cure, J. Non-Newtonian Fluid Mech. 56 (1995) 221-251. doi:10.1016/0377-0257(94)01282-M.

[26] E.A. Abdel-Aal, M.M. Rashad, H. El-Shall, Crystallization of calcium sulfate dihydrate at different supersaturation ratios and different free sulfate concentrations, Crystal Res. & Tech. 39 (2004) 313-321. https://doi.org/10.1002/crat.200310188

[27] S. Kratz, J. Schick, E. Schnug, Trace elements in rock phosphates and P containing mineral and organo-mineral fertilizers sold in Germany, Sci. Total Environ. 542B (2016) 1013-1019. https://doi.org/10.1016/j.scitotenv.2015.08.046

[28] M. Contreras, R. Pérez López, M.J. Gázquez, V. Morales-Flórez, A. Santos, L. Esquivias, J.P. Bolívar, Fractionation and fluxes of metals and radionuclides during the recycling process of phosphogypsum wastes applied to mineral CO_2 sequestration, Waste Manag. 45 (2015) 412-419. https://doi.org/10.1016/j.wasman.2015.06.046

[29] C.H.R. Saueia, F.M. Le Bourlegat, B.P. Mazzilli, D.I.T. Fávaro, Availability of metals andradionuclides present in phosphogypsum and phosphate fertilizers used in Brazil. J. Radioanalytical and Nuclear Chem. 297 (2012) 189-195. https://doi.org/10.1007 / s10967-012-2361-2

[30] J.P. Wang, E. Gallo, B. François, F. Gabrieli, P. Lambert, Capillary force and rupture of funicular liquid bridges between three spherical bodies, Powder Technology, 305 (2017) 89–98. http://dx.doi.org/10.1016/j.powtec.2016.09.060

[31] P. Coussot, Yield stress fluid flows: A review of experimental data, J. Nonnewton. Fluid Mech., 211 (2014) 31-49. https://doi.org/10.1016/j.jnnfm.2014.05.006

[32] J. Mewis, Thixotropy, general review. J. Nonnewton. Fluid Mech., 6 (1979) 1-20. https://doi.org/10.1016/0377-0257(79)87001-9

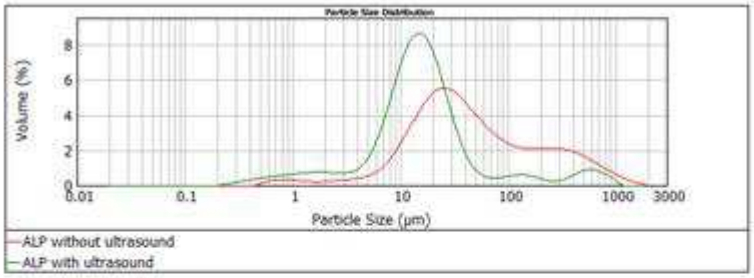

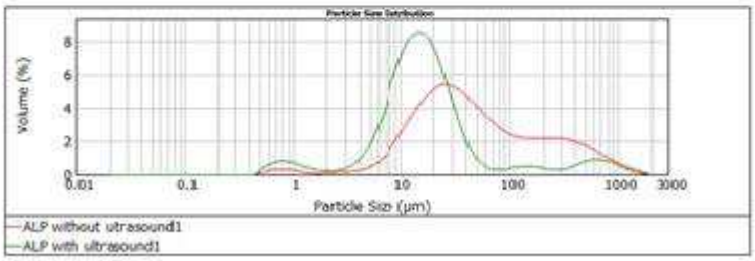

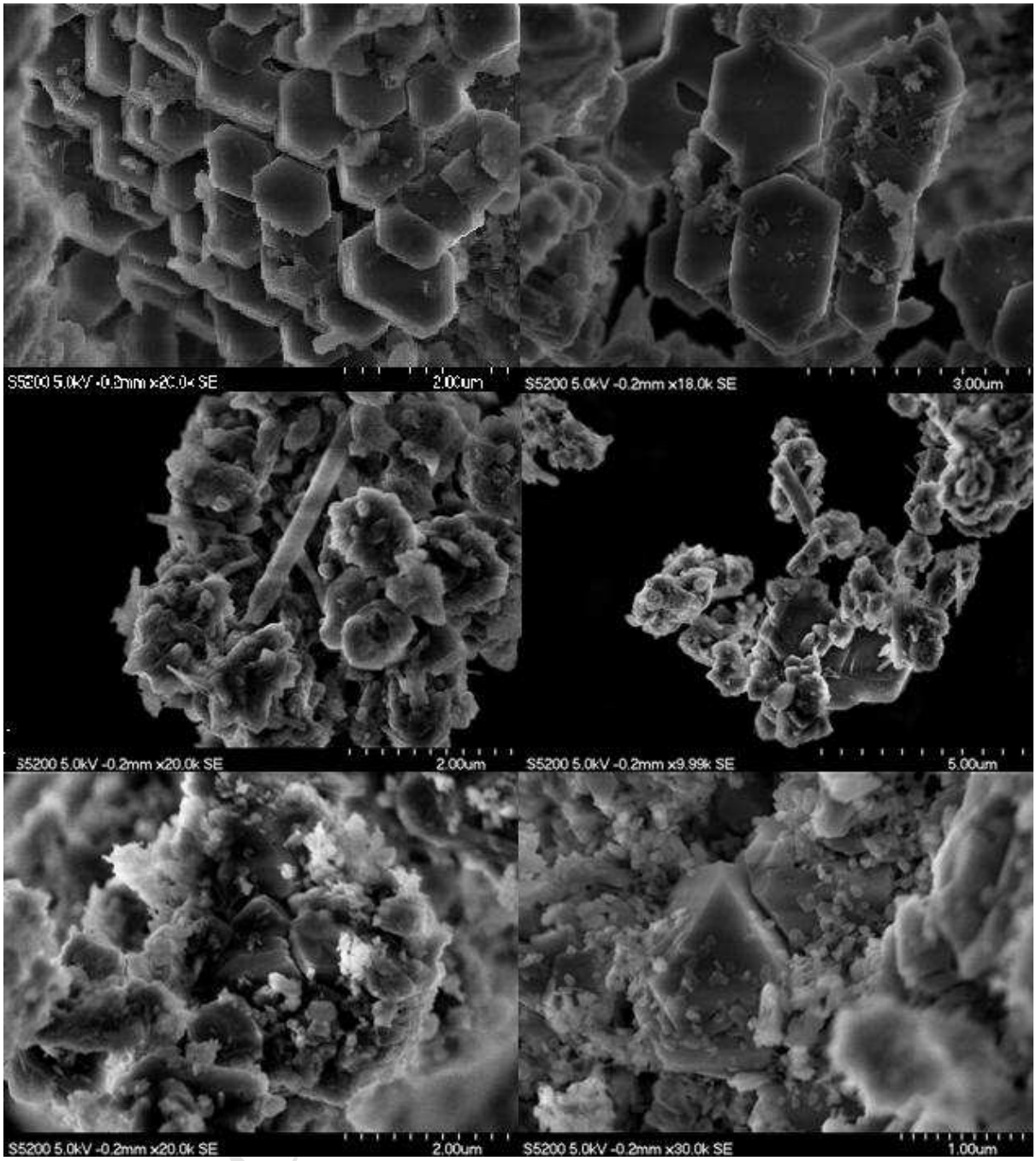
S5200 5.0kV -0.2mm x20.0k SE
2.00um
S5200 5.0kV -0.2mm x18.0k SE
3.00um
S5200 5.0kV -0.2mm x20.0k SE
2.00um
S5200 5.0kV -0.2mm x9.99k SE
5.00um
S5200 5.0kV -0.2mm x20.0k SE
2.00um
S5200 5.0kV -0.2mm x30.0k SE
1.00um

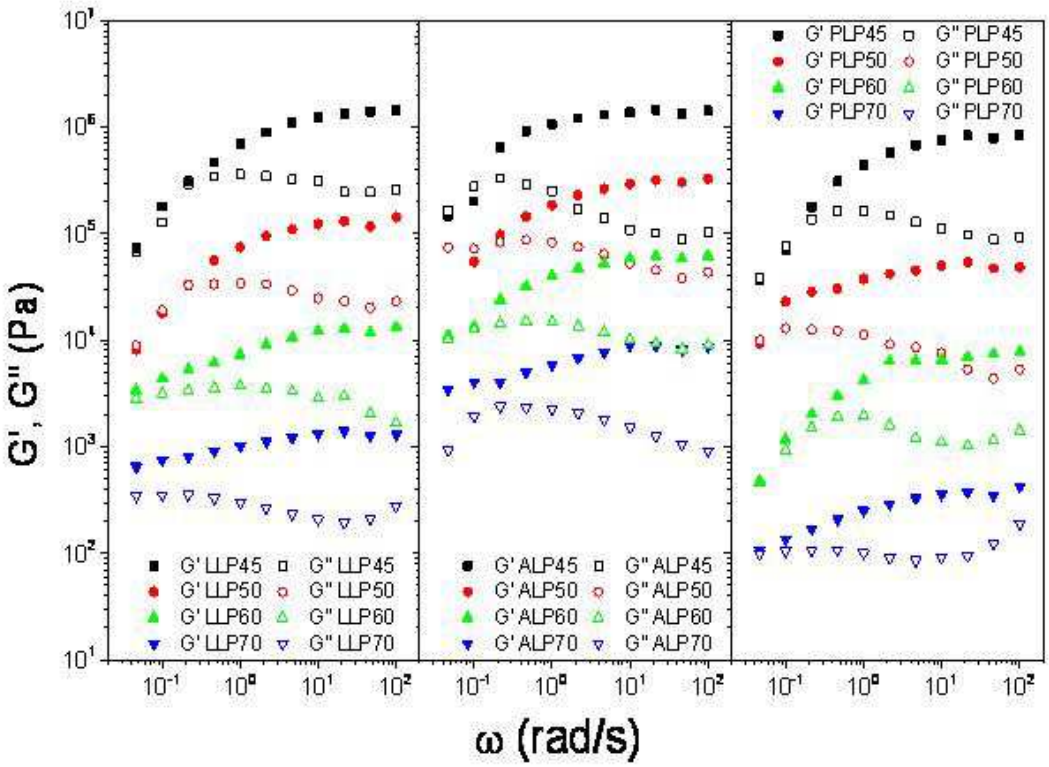

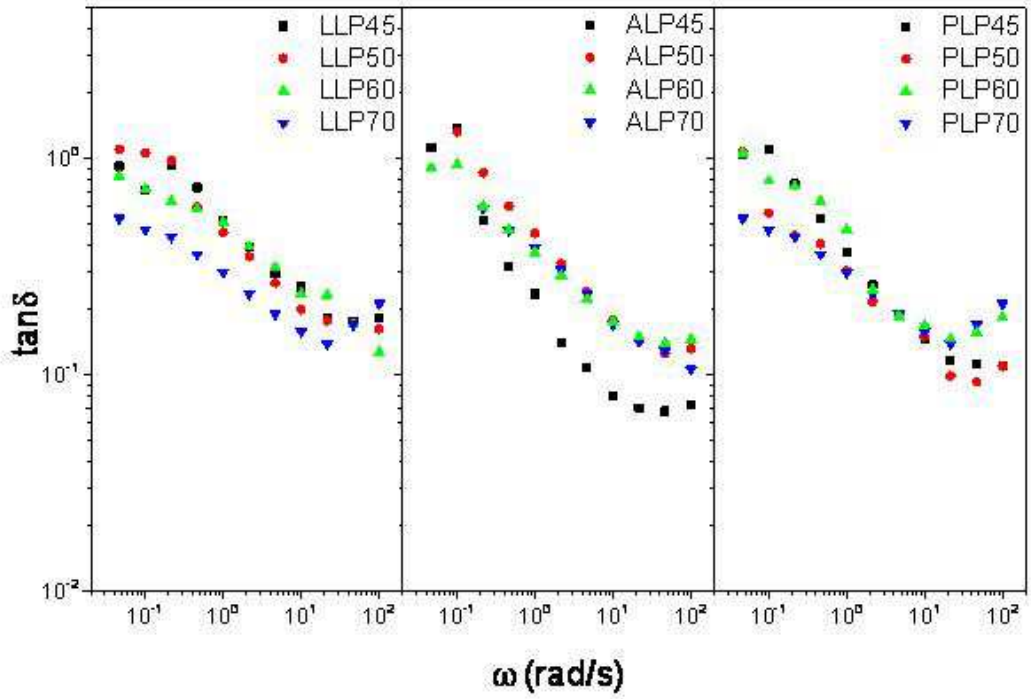

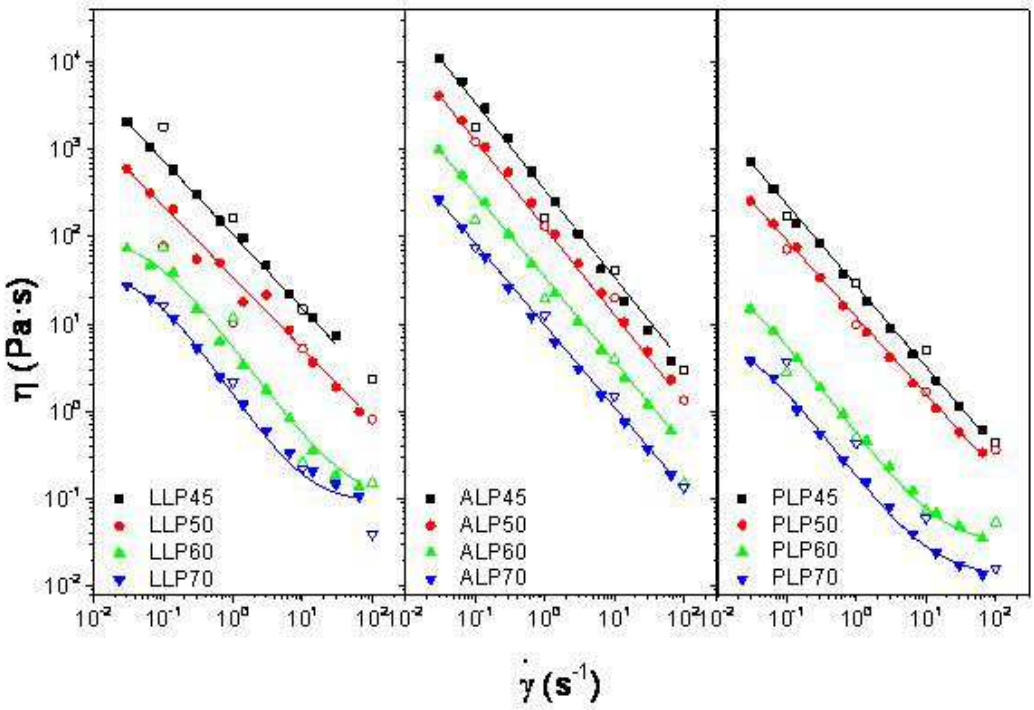

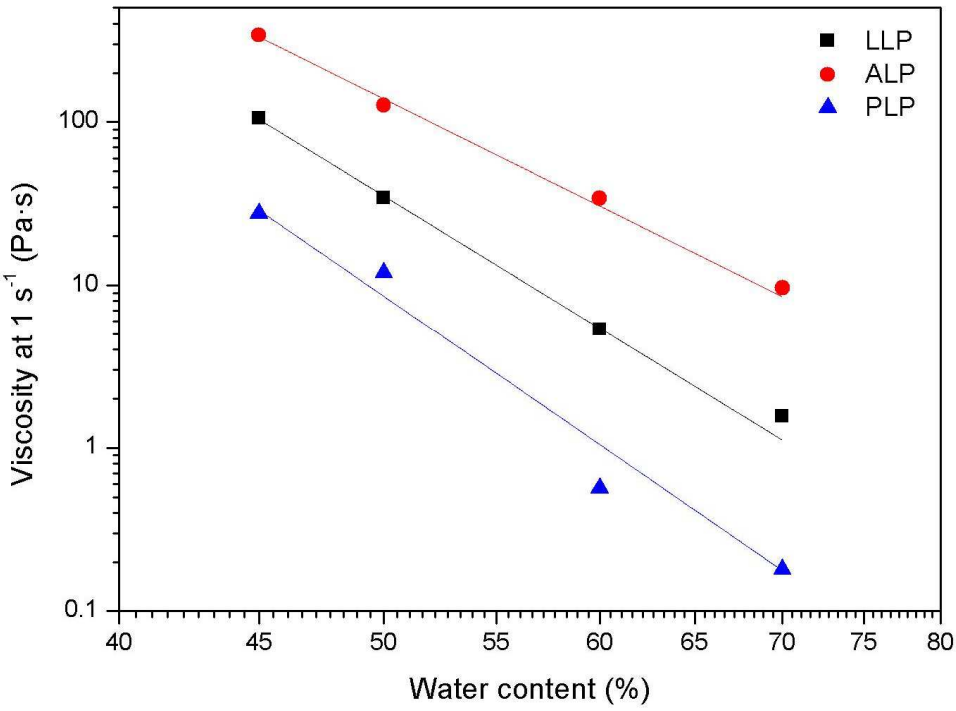

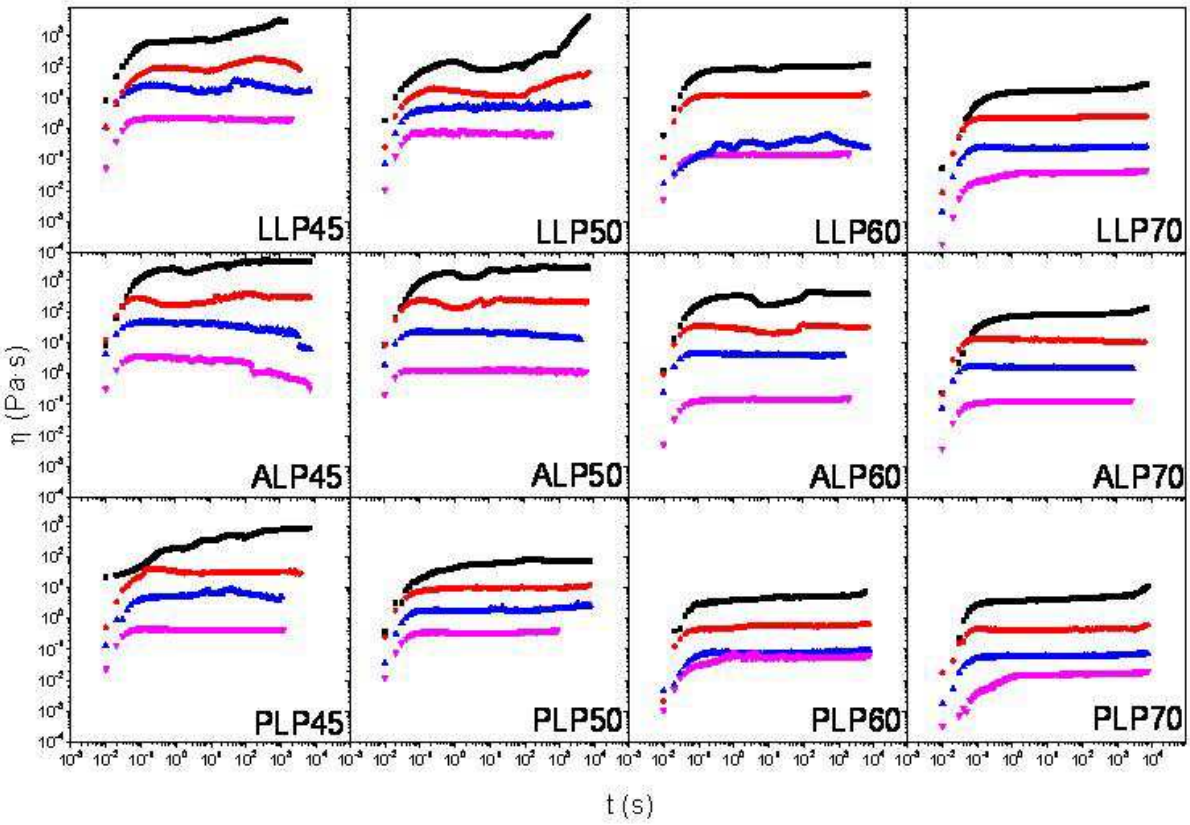

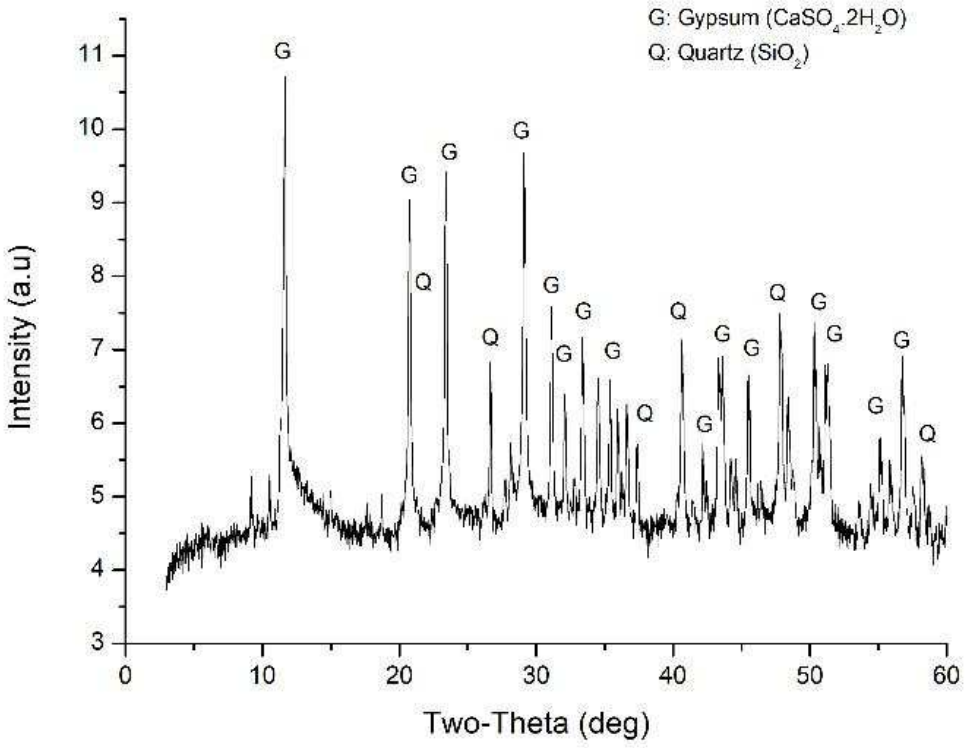

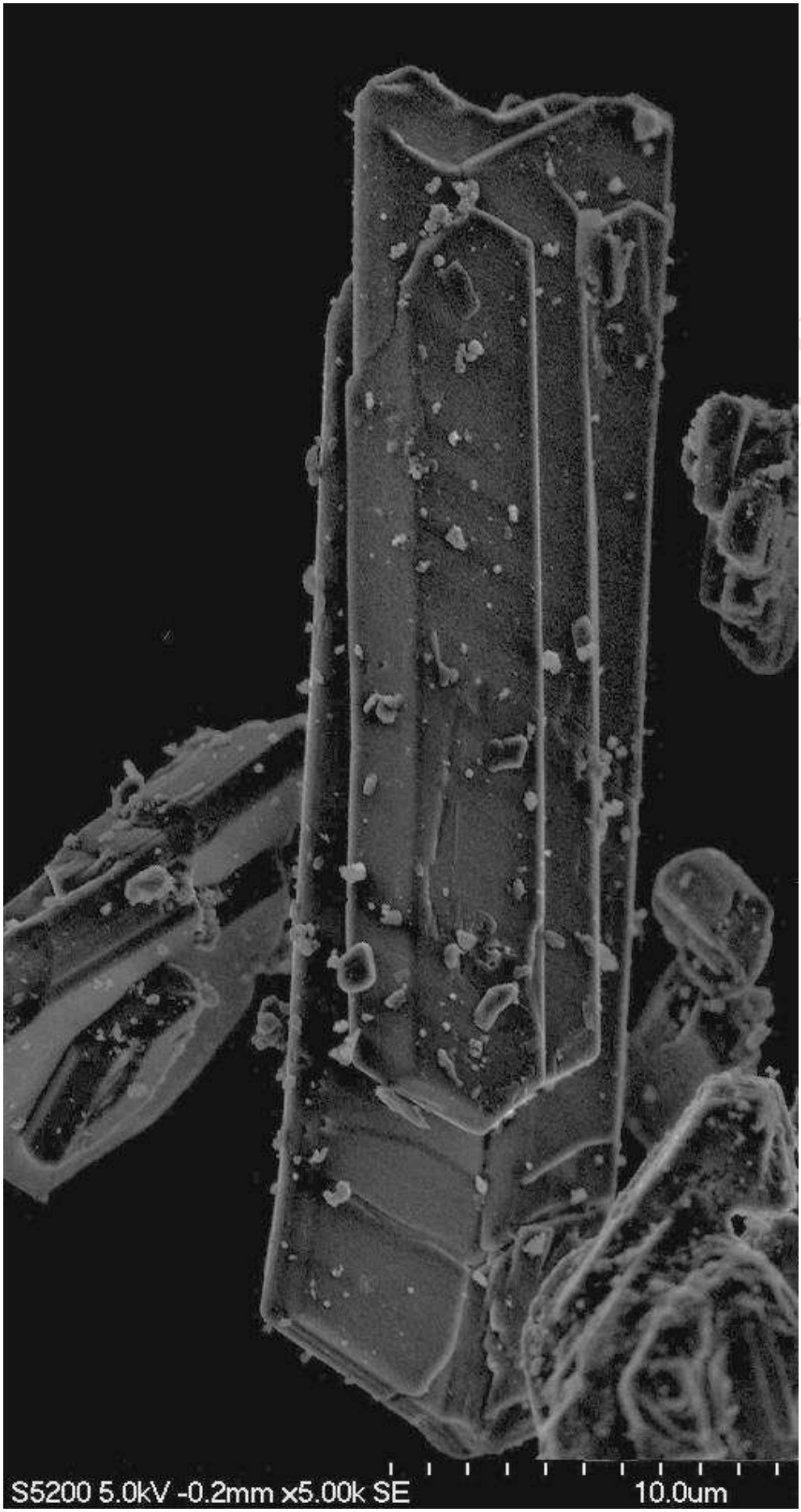
S5200 5.0kV -0.2mm x5.00k SE
10.0um